

## CHAPTER 4

### DESIGN FUNDAMENTALS OF SHELL-AND-TUBE HEAT EXCHANGERS

#### 4.1 INTRODUCTION

The thermal design of heat exchangers is directed to calculate an adequate surface area to handle the thermal duty for the given specifications whereas the hydraulic analysis determines the pressure drop of the fluids flowing in the system, and consequently the pumping power or fan work input necessary to maintain the flow.

The most common problems in heat exchanger design are rating and sizing. The *rating* problem is evaluating the thermo-hydraulic performance of a fully specified exchanger. The rating program determines the heat transfer rate and the fluid outlet temperatures for prescribed fluid flow rates, inlet temperatures, and the pressure drop for an existing heat exchanger; therefore the heat transfer surface area and the flow passage dimensions are available. The rating program is shown schematically in Figure 4.1. [2] The *sizing* problem, however, is concerned with the determination of the dimensions of the heat exchanger. In the sizing problem, an appropriate heat exchanger type is selected and the size to meet the specified hot and cold fluid inlet and outlet temperatures, flow rates, and pressure drop requirements, is determined.

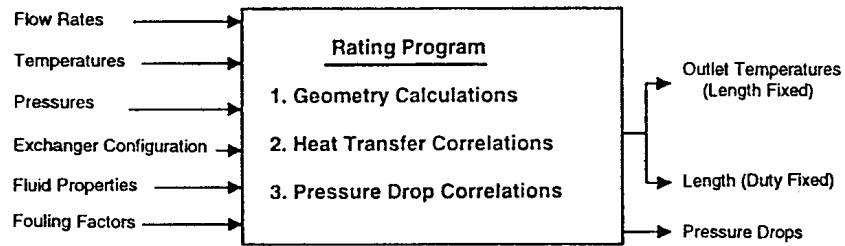


Figure 4.1 The rating program

There are some criteria for a successful heat exchanger design. These principles are given below. [2]

- The process requirements which are accomplishing the thermal change on the streams within the allowable pressure drops, and retaining the capability to do this in the presence of fouling until the next scheduled maintenance period must be fulfilled.
- The heat exchanger must withstand the service conditions of the plant environment.
- The exchanger must be maintainable. In other words, a configuration that permits cleaning and replacement of any component that is especially vulnerable to corrosion, erosion, vibration, or aging, must be chosen.
- The designer should consider the advantages of a multishell arrangement with flexible piping and valving provided to allow one unit to be taken out of service for maintenance without disturbing the rest of the plant.
- The heat exchanger should cost as little as possible provided that the above criteria are satisfied.
- Limitations on the heat exchanger length, diameter, weight, and/or tube specifications due to site requirements, lifting and servicing capabilities must be all taken into consideration in the design.

There are some terms used in heat exchanger specification problems and their solutions, which are often confused. These are ‘rating’, ‘design’, and ‘selection’. ‘*Rating*’ is the computational process in which the inlet flow rates and

temperatures, the fluid properties, and the heat exchanger parameters are taken as input and the outlet temperatures and thermal duty (if the exchanger length is specified) or the required length of the heat exchanger are calculated as output. In either case, the pressure drop of each stream will also be calculated. *Design* is the process of determining all essential constructional dimensions of an exchanger that must perform a given heat duty and respect limitations on shell-side and tube-side pressure drop. A number of other criteria are also specified, such as minimum or maximum flow velocities, ease of cleaning and maintenance, erosion, size and/or weight limitations, tube vibration, and thermal expansion. Each design problem has a number of potential solutions, but only one will have the best combination of characteristics and cost. *Selection* means choosing a heat exchanger from among a number of units already existing. Typically, these are standard units listed in catalogs of various manufacturers. Sufficient manufacturer's data usually exist to allow one to select comfortably oversized exchanger with respect to both area and pressure drop.

For the present chapter, Kern and Bell-Delaware methods will be presented by performing Thermal Analysis and Hydraulic Analysis separately for the tube-side and for the shell-side. The rationale behind these choices is that the Kern method offers the simplest route and the Bell-Delaware method offers the most widely accepted method.

## **4.2 KERN METHOD**

The first attempts to provide methods for calculating shell-side pressure drop and heat transfer coefficient were those in which correlations were developed based on experimental data for typical heat exchangers. One of these methods is the well-known Kern method, which was an attempt to correlate data for standard exchangers by a simple equation analogous to equations for flow in tubes. However, this method is restricted to a fixed baffle cut (25%) and cannot adequately account for baffle-to-shell and tube-to-baffle leakages. However, although the Kern equation is not particularly accurate, it does allow a very simple and rapid calculation of shell-side coefficients and pressure drop to be carried out

and has been successfully used since its inception. [1]

Since Delaware method is a rating analysis, first Kern method is used to estimate the size of the heat exchanger for a given specification.

#### 4.2.1 Thermal Analysis for Tube-Side

##### 4.2.1.1 Number of Tubes

The flow rate inside the tube ( $\dot{m}_t$ ) is a function of the density of the fluid ( $\rho_t$ ), the velocity of the fluid ( $u_t$ ), cross-sectional flow area of the tube ( $A_c$ ), and the number of tubes ( $N_t$ ). [4]

$$\dot{m}_t = \rho_t u_t A_c N_t \quad (4.1)$$

By using Eq. (4.1) and replacing  $A_c$  by  $\pi d_i^2 / 4$ , number of tubes can be calculated as

$$N_t = \frac{4\dot{m}_t}{\rho_t u_t \pi d_i^2} \quad (4.2)$$

where  $d_i$  is the tube inside diameter.

##### 4.2.1.2 Tube-Side Reynolds Number

The criterion of distinguishing between laminar and turbulent flow is the observed mixing action. Experiments have shown that laminar flow exists when the Reynolds number (Re) is less than 2000. [4]

$$\text{Re}_t = \frac{\rho_t u_t d_i}{\mu_t} \quad (4.3)$$

where  $\mu_t$  is the viscosity of the tube-side fluid,  $u_t$  is fluid velocity inside the tubes, and  $\rho_t$  is the density of fluid in the tubes.

#### 4.2.1.3 Tube-Side Nusselt Number

Nusselt number is a function of Reynolds number (Re) and Prandtl number (Pr). However, there are equations developed according to the type of flow. For turbulent flow, the following equation developed by Petukhov-Kirillov can be used. [47]

$$Nu_t = \frac{(f/2)Re_t Pr_t}{1.07 + 12.7(f/2)^{1/2}(Pr_t^{2/3} - 1)} \quad (4.4)$$

where  $f$  is the friction factor which can be calculated from

$$f = (1.58 \ln Re_t - 3.28)^{-2} \quad (4.5)$$

Eq. (4.4) predicts the results in the range  $10^4 < Re_t < 5 \times 10^6$  and  $0.5 < Pr_t < 200$  with 5 to 6% error, and in the range  $0.5 < Pr_t < 2000$  with 10% error.

For laminar flow, the Sieder and Tate correlation can be used. [48]

$$Nu_t = 1.86 \left( \frac{Re_t Pr_t d_i}{L} \right)^{1/3} \quad (4.6)$$

where  $Re_t$  is the Reynolds number for the tube-side,  $Pr_t$  is the Prandtl number for the tube-side fluid,  $d_i$  is the tube inside diameter, and  $L$  is the tube length. Eq. (4.6) is applicable for  $0.48 < Pr_t < 16700$  and  $(Re_t Pr_t d_i/L)^{1/3} > 2$ .

#### 4.2.1.4 Tube-Side Heat Transfer Coefficient

The heat transfer coefficient for the tube-side is expressed as follows:

$$h_t = Nu_t \frac{k_t}{d_i} \quad (4.7)$$

where  $Nu_t$  is the Nusselt number for the tube-side fluid which is found by using Eqs. (4.4) and (4.6),  $k_t$  is the thermal conductivity of the tube-side fluid, and  $d_i$  is the tube inside diameter.

#### 4.2.2 Thermal Analysis for Shell-Side

##### 4.2.2.1 Shell Diameter

The number of tubes is calculated by taking the shell circle and dividing it by the projected area of the tube layout. That is [5]

$$N_t = (CTP) \frac{\pi D_s^2}{4A_1} \quad (4.8)$$

where  $A_1$  is the projected area of the tube layout expressed as area corresponding to one tube (Eq. 4.9),  $D_s$  is the shell inside diameter, and  $CTP$  is the tube count calculation constant that accounts for the incomplete coverage of the shell diameter by the tubes, due to necessary clearances between the shell and the outer tube circle and tube omissions due to tube pass lanes for multitude pass design [5]. The  $CTP$  values for different tube passes are given below: [5]

one-tube pass	→	$CTP = 0.93$
two-tube pass	→	$CTP = 0.90$
three-tube pass	→	$CTP = 0.85$

$A_1$  is expressed as

$$A_1 = (CL)P_T^2 \quad (4.9)$$

where  $P_T$  is the tube pitch and  $CL$  is the tube layout constant.

$$\begin{aligned} \text{for } 90^\circ \text{ and } 45^\circ & \rightarrow CL = 1.0 \\ \text{for } 30^\circ \text{ and } 60^\circ & \rightarrow CL = 0.87 \end{aligned}$$

Combining Eq. (4.8) with Eq. (4.9), one gets

$$N_t = \frac{\pi(CTP)D_s^2}{4(CL)(PR)^2(d_o)^2} \quad (4.10)$$

where  $PR$  is the tube pitch ratio given by

$$PR = \frac{P_T}{d_o} \quad (4.11)$$

In Eq. (4.11),  $d_o$  is the tube outside diameter. The shell inside diameter  $D_s$  from Eq. (4.10) can be written as [5]

$$D_s = 0.637 \sqrt{\frac{CL}{CTP} \left[ \frac{A_o(PR)^2 d_o}{L} \right]^{1/2}} \quad (4.12)$$

where  $A_o$  is the outside heat transfer surface area based on the outside diameter of the tube and can be calculated by the following formula

$$A_o = \pi d_o N_t L \quad (4.13)$$

### 4.2.2.2 Shell Equivalent Diameter

The equivalent diameter is calculated along (instead of across) the long axes of the shell and therefore is taken as four times the net flow area as layout on the tube sheet (for any pitch layout) divided by the wetted perimeter. [1]

$$D_e = \frac{4 \times \text{free-flow area}}{\text{wetted perimeter}} \quad (4.14)$$

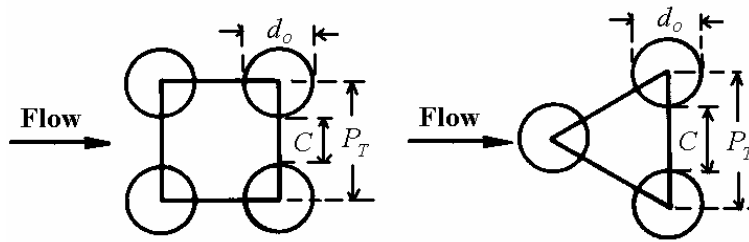


Figure 4.2 Square and triangular pitch-tube layouts

As shown in Figure 4.2 [5], for the square pitch, the perimeter is the circumference of a circle and the area is a square of pitch size ( $P_T^2$ ) minus the area of a circle. Therefore, for a square pitch (as if flow is parallel to the axis of the heat exchanger): [1]

$$D_e = \frac{4(P_T^2 - \frac{\pi d_o^2}{4})}{\pi d_o} \quad (4.15)$$

and for the triangular pitch: [1]

$$D_e = \frac{4\left(\frac{P_T^2 \sqrt{3}}{4} - \frac{\pi d_o^2}{8}\right)}{\pi d_o / 2} \quad (4.16)$$

where  $d_o$  is the tube outside diameter.

The number of tubes at the centerline of the shell is calculated by

$$N_t = \frac{D_s}{P_T} \quad (4.17)$$

where  $N_t$  is the number of tubes and  $P_T$  is the tube pitch and the flow area associated with each tube between baffles is  $(C \cdot B)$ ; hence

$$A_s = \frac{D_s}{P_T} C B \quad (4.18)$$

where  $A_s$  is the bundle cross flow area,  $D_s$  is the inner diameter of the shell,  $C$  is the clearance between adjacent tubes, and  $B$  is the baffle spacing. As shown in Figure 4.2, the tube clearance ( $C$ ) is expressed as

$$C = P_T - 2r_o = P_T - d_o \quad (4.19)$$

Then the shell-side mass flow rate is found with

$$G_s = \frac{\dot{m}_s}{A_s} \quad (4.20)$$

where  $\dot{m}_s$  is the flow rate of the shell-side fluid.

#### 4.2.2.3 Shell-Side Reynolds Number

Reynolds number for the shell-side is based on the tube diameter and the velocity on the cross flow area at the diameter of the shell:

$$\text{Re}_s = \left( \frac{\dot{m}_s}{A_s} \right) \frac{D_e}{\mu_s} \quad (4.21)$$

where  $D_e$  is the equivalent diameter on the shell-side,  $\dot{m}_s$  is the flow rate of the shell-side fluid,  $\mu_s$  is the viscosity of the shell-side fluid, and  $A_s$  is the cross flow area at the shell diameter.

#### 4.2.2.4 Shell-Side Heat Transfer Coefficient

The heat transfer coefficient for the shell-side in the *Kern Method* can be estimated from [1]

$$h_o = \frac{0.36k_s}{D_e} \text{Re}_s^{0.55} \text{Pr}_s^{1/3} \quad (4.22)$$

$$\text{for } 2 \times 10^3 < \text{Re}_s = \frac{G_s D_e}{\mu} < 1 \times 10^6$$

where  $k_s$  is the thermal conductivity of the shell-side fluid,  $\text{Re}_s$  is the Reynolds number for the shell-side,  $\text{Pr}_s$  is the Prandtl number for the shell-side fluid, and  $D_e$  is the equivalent diameter on the shell-side.

#### 4.2.2.5 Overall Heat Transfer Coefficient for the Heat Exchanger

The overall heat transfer coefficient for clean surface ( $U_c$ ) is given by

$$\frac{1}{U_c} = \frac{1}{h_o} + \frac{1}{h_i} \frac{d_o}{d_i} + \frac{r_o \ln(r_o/r_i)}{k} \quad (4.23)$$

where  $h_o$  is the shell-side heat transfer coefficient,  $h_i$  is the tube-side heat transfer coefficient,  $r_o$  is the tube outer radius,  $r_i$  is the tube inner radius, and  $k$  is the thermal conductivity of the tube material.

Considering the total fouling resistance  $R_{ft}$  given in Table D.1 [36], the heat transfer coefficient for fouled surface ( $U_f$ ) can be calculated from the following expression:

$$\frac{1}{U_f} = \frac{1}{U_c} + R_{ft} \quad (4.24)$$

#### 4.2.2.6 Outlet Temperature Calculation and Length of the Heat Exchanger

The amount of heat exchange between two fluids as they flow through a one shell-pass, two tube-passes shell-and-tube heat exchanger due to temperature variation is given in Eqs. (3.5), (3.6), and (3.7). By equating Eqs. (3.5) and (3.6), the outlet temperature for the fluid flowing through the tube is

$$T_{c2} = \frac{(\dot{m}c_p)_h(T_{h1} - T_{h2})}{(\dot{m}c_p)_c} + T_{c1} \quad (4.25)$$

The log-mean temperature difference  $LMTD$  can be calculated by using Eq. (3.25). Since the total heat transfer rate is also known, the surface area of the heat exchanger for the fouled condition is

$$A_f = \frac{Q}{U_f(F)(LMTD)} \quad (4.26a)$$

and for the clean condition

$$A_c = \frac{Q}{U_c(F)(LMTD)} \quad (4.26b)$$

where the  $LMTD$  is always for the counter flow,

$$LMTD = \frac{(T_{h1} - T_{c2}) - (T_{h2} - T_{c1})}{\ln[(T_{h1} - T_{c2}) / (T_{h2} - T_{c1})]} \quad (4.27)$$

The over surface design (OS) can be calculated from [1]

$$OS = \frac{A_f}{A_c} = \frac{U_c}{U_f} \quad (4.28)$$

The corresponding total resistance will be from Eq. (4.24)

$$R_{ft} = \frac{1}{U_f} - \frac{1}{U_c} \quad (4.29)$$

The length of the heat exchanger is calculated by

$$L = \frac{A_f}{N_t \pi d_o} \quad (4.30)$$

where  $N_t$  is the total number of the tubes,  $d_o$  is the tube outer diameter, and  $L$  is the length of the heat exchanger.

#### 4.2.2.7 Shell Diameter

Shell diameter can be recalculated from Eq. (4.12) as [5]

$$D_s = 0.637 \sqrt{\frac{CL}{CTP} \left[ \frac{A_f (PR)^2 d_o}{L} \right]^{1/2}} \quad (4.31)$$

where  $CL$  and  $CTP$  values for different tube passes and tube layouts are given in section 4.2.2.1.

### 4.2.3 Hydraulic Analysis for Tube-Side

The pressure drop encountered by the fluid making  $N_p$  passes through the heat exchanger is a multiple of the kinetic energy of the flow. Therefore, the tube-side pressure drop is calculated by [4, 6]

$$\Delta p_t = \left( 4f_t \frac{LN_p}{d_i} + 4N_p \right) \frac{\rho_t u_t^2}{2} \quad (4.32)$$

where  $L$  is the tube length,  $N_p$  is the number of passes,  $\rho_t$  is the density of the fluid flowing inside the tubes, and  $f_t$  is the friction factor calculated from Eq. (4.5). The second term in Eq. (4.32) which is  $4N_p \frac{\rho_t u_t^2}{2}$  is the additional pressure drop introduced by the change of direction in the passes. The tube fluid experiences sudden expansions and contractions during a return that is accounted for allowing four velocity heads per pass.

### 4.2.4 Hydraulic Analysis for Shell-Side

The shell-side fluid experiences a pressure drop as it passes through the exchanger, over the tubes, and around the baffles. If the shell fluid nozzles (inlet and outlet ports) are on the same side of the heat exchanger, then the shell-side fluid makes an even number of the tube bundle crossings, but if they are on opposite sides, then it makes an odd number of the bundle crossings. The number of bundle crossings therefore influences the pressure drop. Based on experiment, the pressure drop experienced by the shell-side fluid is calculated by [1,6]

$$\Delta p_s = \frac{f_s G_s^2 (N_b + 1) D_s}{2 \rho_s D_e \phi_s} \quad (4.33)$$

where  $\phi_s = (\mu_b / \mu_w)^{0.14}$ ,  $N_b$  is the number of baffles,  $(N_b + 1)$  is the number of

times the shell fluid passes the tube bundle,  $D_e$  is the shell equivalent diameter determined from Eqs. (4.14) and (4.15),  $\rho_s$  is the density of the shell-side fluid, and  $D_s$  is the shell inner diameter. The friction factor,  $f_s$ , for the shell is calculated from [1, 6]

$$f_s = \exp(0.576 - 0.19 \ln \text{Re}_s) \quad (4.34)$$

where

$$400 < \text{Re}_s = \frac{G_s D_e}{\mu} \leq 1 \times 10^6$$

Note that  $\mu_b$  is the viscosity of the shell-side fluid at bulk temperature, and  $\mu_w$  is the viscosity of the tube-side fluid at wall temperature. The wall temperature can be calculated as follows:

$$T_w = \frac{1}{2} \left( \frac{T_{c1} + T_{c2}}{2} + \frac{T_{h1} + T_{h2}}{2} \right)$$

### 4.3 BELL-DELAWARE METHOD

#### 4.3.1 Historical Development of the Delaware Method

The Department of Chemical Engineering at the University of Delaware started in 1947, a comprehensive research program on shell-side design of shell-and-tube heat exchangers. This project is called Delaware Project and it finished in 1963. In 1947, the project started under ASME sponsorship using funds from the Tubular Exchanger Manufacturers Association, the American Petroleum Institute, Standard Oil Development Co., Andale Company, Downingtown Iron Works, Davis Engineering Co., E.I. du Pont de Nemours and Company, and York Corporation. The principal investigators were Professors Olaf Bergelin and Allan Colburn of the University of Delaware. [2]

In 1947, the experimental program started with measurements of heat transfer and pressure drop during flow across ideal tube banks and hence the various design features characteristic of shell-and-tube heat exchangers were introduced in commercial use. Then several baffle cut and spacing configurations were studied inside a cylindrical shell with no baffle leakage first. But baffle leakages between baffles and the shell and between the tubes and baffles were added afterwards. Finally, the bypass flow around the bundle between the outer tube limit and the shell inner diameter was investigated. The first report was published in 1950 and the second report, in 1958. In 1960, a preliminary design method for E shell heat exchangers was issued. In 1963, the final report was published. [2]

#### **4.3.2 Simplified Mechanisms of Shell-Side Flow**

As can be seen from Figure 4.3 [6], five different streams are identified on the shell-side. Stream B is the main cross flow stream flowing through one window across the cross flow section and out through the opposite window.

However, there are four other streams because of the mechanical clearances required in a shell-and-tube heat exchanger. One of them is the A stream that leaks through the clearance between the tubes and the baffle, from one baffle compartment to the next. There is also the C stream which is the bundle bypass stream and which flows around the tube bundle between the outermost tubes in the bundle and the inside of the shell. The E stream flows through the clearance between the baffles and the inside diameter of the shell. Finally, the F stream flows through any channels within the tube bundle caused by the provision of pass dividers in the exchanger header. Therefore, it exists only in multiple tubepass configurations.

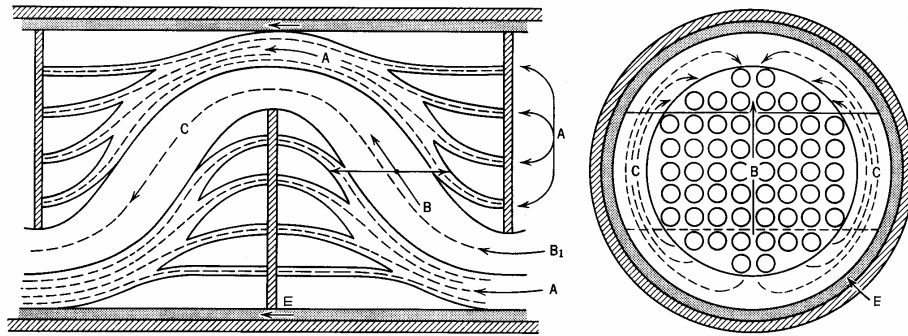


Figure 4.3 Diagram indicating leaking paths for flow bypassing the tube matrix, both through the baffle clearances between the tube matrix and shell

Figure 4.3 is an idealized representation of course because the streams defined above are not exactly as they are shown in the figure. They form and mix and interact with one another and a more complete analysis is needed for the shell-side flow but this analysis cannot be carried out exactly because of a lack of knowledge of the turbulent flow structures on the shell-side.

All the streams other than B affect the performance of the essential B stream. The first effect of the various streams is that they reduce the B stream and therefore the local heat transfer coefficient. Secondly, they change the shell-side temperature profile. The Delaware method lumps these two effects together into a single correction.

Bell (1963) [1] developed therefore Delaware method in which correction factors were introduced for the following elements:

- (a) Leakage through the gaps between the tubes and the baffles and the baffles and the shell, respectively.
- (b) Effect of the baffle configuration (i.e., a recognition of the fact that only a fraction of the tubes are in pure cross flow).
- (c) Bypassing of the flow around the gap between the tube bundle and the shell.
- (d) Effect of adverse temperature gradient on heat transfer in laminar flow.

Delaware method is a rating analysis. In a rating problem, the process specifications which are the flow rates, outlet temperatures (if length is to be found), inlet temperatures, physical properties, fouling characteristics, and geometrical parameters of the heat exchanger which are the shell inside diameter, the outer tube limit, the tube diameter, the tube layout, the baffle spacing and the baffle cut are all given and the length (if not given) and the duty (if length is given) and pressure drops for both cases are calculated. [37]

### 4.3.3 Basic Input Data

To rate the heat exchanger, the input data should be fully specified. [3] The basic set of input data is required for shell-side rating calculations. It includes data for the design of the overall exchanger, including tube-side flow and some values (such as leakage and bypass clearances) that are not readily available and usually must be estimated. Basic data required for tube-side calculations are also included, as they must form an entity of the entire shell-and-tube heat exchanger rating process. Moreover, tube-side data enter directly into shell-side flow calculations in several aspects, for example, tube wall temperature, tube count, etc.

The TEMA Standards [36] are used wherever applicable, but metric (DIN) standards are introduced wherever possible.

The following list shows all the basic input data with the comments.

- 1)  **$D_s$  (mm), shell inside diameter:** The shell inside diameter value found before in Kern method (or other methods) is used as the input data in the Bell-Delaware method or Tables E.1-E.3 [3] show suggested dimensional series for inch-based U.S. practice and for metric as per DIN 28008 and other industrial standards.
- 2)  **$d_o$  (mm), tube outside diameter:** Tables E.4 and E.5 [3] show the

recommended tube dimensions in inch standard and in metric standard, respectively.

There are some criteria to be used while selecting the tube diameter. Small tube diameters are generally preferred because of better heat transfer effectiveness, but cleaning considerations limit the selection of tube diameter. Moreover, the ratio of the tube outside diameter to shell inside diameter must be maintained within reasonable limits. Smaller diameter tubes within larger shells would not be economically justifiable. In the same way, relatively large tube diameters in small shells cause the correlational parameter effects to be faulty. Therefore the approximate ratio of minimum  $D_s$  to  $d_o$  should generally be about 15. [3]

3)  **$L_{tw}$  (mm), tube wall thickness:** Tube wall thickness is determined according to temperature, pressure, material strength, and possible corrosion allowance from standard practice. Tube wall thickness is used in the determination of inside tube diameter  $d_i$  and in tube wall resistance calculations.

4)  **$d_i$  (mm), tube inside diameter:** Tables E.4 and E.5 show the nominal values of tube inside diameters. Tube inside diameter is calculated as

$$d_i = d_o - 2(L_{tw}) \quad (4.35)$$

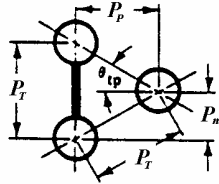
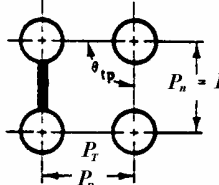
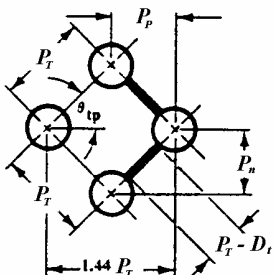
5)  **$k$  (W/m.K), tube wall material thermal conductivity:** The thermal conductivity of the tube wall material is used in the determination of the tube wall heat transfer resistance. The value of tube wall material thermal conductivity is dependent on temperature and can be found from material properties tables.

6)  **$P_T$  (mm), tube layout pitch:** The tube layout pitch is used in the determination of the cross flow area. The smaller the value, the more tubes

can be located in a given shell. However, one should pay attention to the minimum necessary distance between adjacent tube holes in the tube-sheet, which is required for proper tube-to-tubesheet joint. Shell-side pressure drop can be adjusted by the tube layout pitch variation. If mechanical cleaning is required on the shell-side, the gap between adjacent tubes should be kept to about ¼ in or 6.3 mm. Tube layout pitch ratio  $P_T/d_o$  which is the ratio of tube pitch to tube diameter should be kept approximately 1.25 as a minimum and 1.5 as a maximum. U.S. practices of tube pitch dimension for specific tube diameters are shown in Table E.6. [3]

- 7)  **$\theta_{tp}$  (deg), tube layout characteristic angle:** The tube layout is defined by the characteristic angle and the corresponding definition of the tube pitch. The tube pitch values for different  $\theta_{tp}$  values are given in Table 4.1. [3]

Table 4.1 Tube layout geometry basic parameters

Cross flow →	$\theta_{tp}$	$P_n$	$P_p$
	30°	$0.5 P_T$	$0.866 P_T$
	90°	$P_T$	$P_T$
	45°	$0.707 P_T$	$0.707 P_T$

The 30°, 45°, and 90° layouts are given but 60° layout is not considered because it produces lower effectiveness in pressure drop to heat transfer conversion for single-phase flow applications and therefore is not generally recommended. The 30° staggered layout has the highest tube density. Therefore, the largest heat transfer surface within a given shell can be obtained by 30° layout. This layout has also a high effectiveness of pressure drop to heat transfer conversion. Therefore, it should be primarily considered while choosing the appropriate tube layout. However, it causes the highest pressure drop for a given tube pitch. The 45° staggered layout has also a high effectiveness of pressure drop to heat transfer conversion. However, when comparing with 30° layout, it is not more advantageous because it permits only about 85% of tubes within a given shell. An important advantage of 45° layout is that the pressure drop for a given pitch is less than for a 30° layout. Another advantage of 45° layout is the possibility of shell-side cleaning from outside by mechanical means, if sufficient clearance between tubes is allowed (approximately 7 mm). The 90° in-line layout should not be used in laminar shell-side flow, but it has also a high effectiveness of pressure drop to heat transfer conversion in turbulent flow. The cleaning convenience of shell-side from outside is the same as for 45° layout. The 90° layout should be considered as an alternative to the 30° or 45° staggered layout, especially if low pressure drop is desired. [37, 3]

- 8)  $L_{to}, L_{ti}, L_{ta}$ , **tube length definitions:** Figure 4.4 [3] shows the tube length definitions.

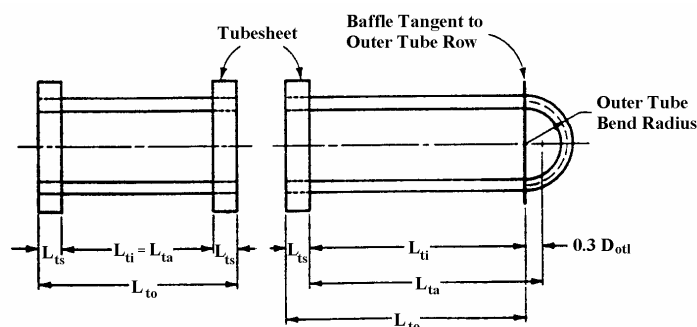


Figure 4.4 Tube length definitions

$L_{to}$  is the nominal tube length for all bundle types except U tubes. For U tube bundles, the tube length varies between the outer and inner rows. The length should be from the tube sheet to the tangent of the outer tube bend. The last baffle should be located at that position.  $L_{ti}$  is the length of summation of all baffle spacings, that is the length between the insides of the tubesheets, except U tubes. For U tubes,  $L_{ti}$  is the distance between the inside of the tube sheet and the last baffle. To determine  $L_{ti}$ , the tubesheet thickness should be known. If the tubesheet thickness is not available, it can be estimated as [3]

$$L_{ts} = 0.1D_s \quad (4.36)$$

with limit  $L_{ts} \geq 25$  mm. The next more accurate estimation of  $L_{ts}$  is [3]

$$L_{ts} = 0.5D_s \sqrt{\frac{P_s}{\sigma_{ts}}} \quad (4.37)$$

where  $P_s$  is the shell-side operating pressure and  $\sigma_{ts}$  is the allowable strength of tubesheet material at operating temperature.  $L_{ti}$  is then calculated as

$$L_{ti} = L_{to} - 2L_{ts} \quad (4.38)$$

for all bundle types except U tubes, and

$$L_{ti} = L_{to} - L_{ts} \quad (4.39)$$

for U tube bundles. Finally,  $L_{ta}$  is the effective tube length for heat transfer area calculations.  $L_{ta}$  is determined as [3]

$$L_{ta} = L_{ti} \quad (4.40)$$

for all bundle types except U tubes, and

$$L_{ta} = L_{ti} + 0.3D_{ol} \quad (4.41)$$

for U tube bundles. [3] For U tube bundles, the tubular area in the U bend beyond the last baffle is estimated as an additional tube length of  $0.3D_{ol}$ , where  $D_{ol}$  is defined in further items. For tube-side pressure drop calculations, the total nominal flow length of the tubes  $L_{tt}$  is required.  $L_{tt}$  is determined as [3]

$$L_{tt} = L_{to} \quad (4.42)$$

for all tube bundle types except U tubes, and

$$L_{tt} = L_{ta} + L_{ts} \quad (4.43)$$

for U tube bundles. [3] Note that these values are multiplied by the number of tube passes  $N_p$  to determine the effective flow length in the tubes.

- 9)  **$B_c$  (%)**, **segmental baffle cut as percent of  $D_s$** : The baffle cut height  $L_{bch}$  (mm) is related to  $B_c$  as shown in Figure 4.5 [3] as

$$B_c = \left( \frac{L_{bch}}{D_s} \right) (100) \quad (\%) \quad (4.44)$$

assuming that the segmental baffle is centered within the shell inside diameter  $D_s$ . The small difference between the shell and baffle diameter is called the clearance  $L_{sb}$  and it is important for leakage corrections. For design purposes and/or for checking on specified values, a chart showing the recommended values, in the form of  $B_c$  versus the ratio of the central baffle spacing  $B$  (which will further be explained) and the inside shell

diameter  $D_s$  is given in Figure 4.6. [3]

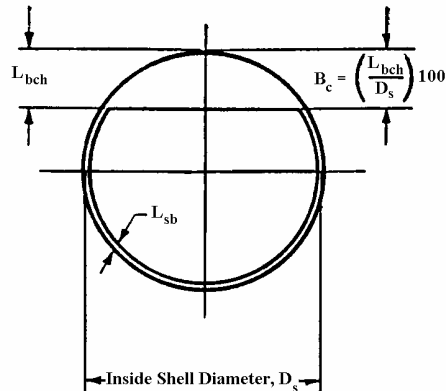


Figure 4.5 Segmental baffle cut height  $L_{bch}$  related to baffle cut  $B_c$  (%)

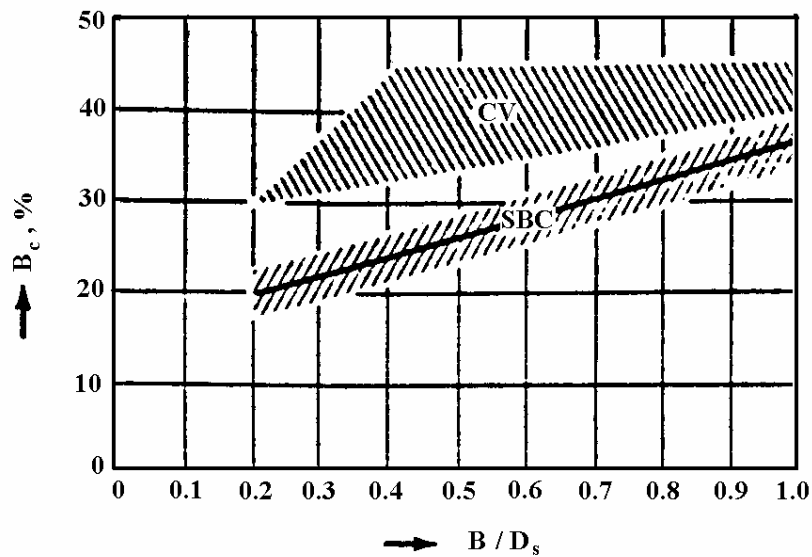


Figure 4.6 Recommended segmental baffle cut values  $B_c$  as a function of  $B/D_s$  ratio. SBC, segmental baffle cuts in no-phase-change flow; CV, baffle cuts applicable to condensing vapors

- 10)  **$B$  (mm), central baffle spacing:** As can be seen from Figure 4.7 [3], the term 'central' in central baffle spacing is to state a uniform baffle spacing



in ( $\approx 6$  mm). The values are represented by the following equations: [3]

Material group A:

$$L_{b,\max} = 52d_o + 532 \quad (\text{mm}) \quad \text{for } d_o = 19 - 51 \text{ mm} \quad (4.45a)$$

$$L_{b,\max} = 68d_o + 228 \quad (\text{mm}) \quad \text{for } d_o = 6 - 19 \text{ mm} \quad (4.45b)$$

Material group B:

$$L_{b,\max} = 46d_o + 436 \quad (\text{mm}) \quad \text{for } d_o = 19 - 51 \text{ mm} \quad (4.45c)$$

$$L_{b,\max} = 60d_o + 177 \quad (\text{mm}) \quad \text{for } d_o = 6 - 19 \text{ mm} \quad (4.45d)$$

Note that for the central baffle spacing, maximum unsupported length is in the baffle window and  $B_{\max} = 0.5L_{b,\max}$ . However, the longest unsupported span can occur in the inlet or outlet baffle spacing and through the adjoining baffle window, as shown in Figure 4.7.

Note that certain shell types such as E, J, and F shell can be used with odd or even number of baffles and hence baffle spacings. For E shell, odd or even number of baffles can be used but nozzle orientation is then determined. However, for J shell, only even number of baffles can be used. In the same way, in F shell, only even number of baffles for standard cross flow orientation is used.

- 11)  **$B_i, B_o$  (mm), inlet and outlet baffle spacing:** In the cases where large inlet and outlet nozzles must be used and the baffle spacing adjoining the nozzles must be enlarged, the additional data entries of  $B_i$  and  $B_o$  are necessary. In these cases the longest unsupported tube span is in the baffle window adjoining the enlarged baffle space. This value must not exceed

the TEMA limitation  $L_{b,max}$  . [3]

- 12)  **$N_t$ , total number of tubes in shell, or number of holes in tubesheet for U tube bundles:** The number of tubes in a tube bundle,  $N_t$ , is a function of shell diameter  $D_s$ , tube bundle type, which in turn affects the value of the ‘tube bundle-to-shell bypass clearance’  $L_{bb}$ , and determines the value of  $D_{ctl}$ , the circle diameter through the centers of the outer tube rows, tube diameter  $d_o$ , tube pitch  $P_T$ , tube layout pattern angle  $\theta_p$ , and number of tube passes  $N_p$ . For heat exchangers specified by drawings or otherwise,  $N_t$  will be known. In most cases it is still important to know if tubes were omitted for impingement plates (Figure 4.8) [3] or bypass partition (Figure 4.9). [3]

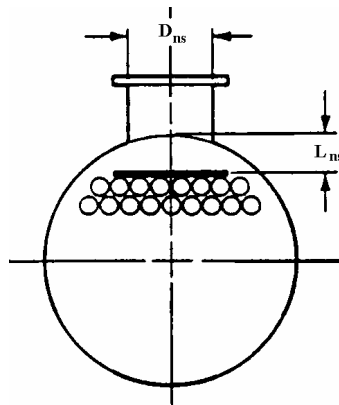


Figure 4.8 Schematic arrangement of shell-side impingement protection

Because of the many parameters affecting  $N_t$ , tabular information based on actual layouts and often referred to as ‘tube count’ is always limited. Especially for design cases where  $D_s$ ,  $N_p$ , and other variables may change while doing the calculations, an estimation procedure is important. A simple but reasonably accurate correlation is suggested below. [3]

For a single tube pass,  $N_p = 1$ :

$$N_t = (N_t)_1 = \frac{0.78D_{ctl}^2}{CL(P_T)^2} \quad (4.46)$$

where  $D_{ctl}$  is the diameter of the circle through the centers of the tube located within the outermost tubes,  $P_T$  is tube layout pitch, and  $CL$  is tube layout constant and  $CL=0.87$  for  $30^\circ$  and  $60^\circ$  layouts or  $CL=1.0$  for  $45^\circ$  and  $90^\circ$  layouts.

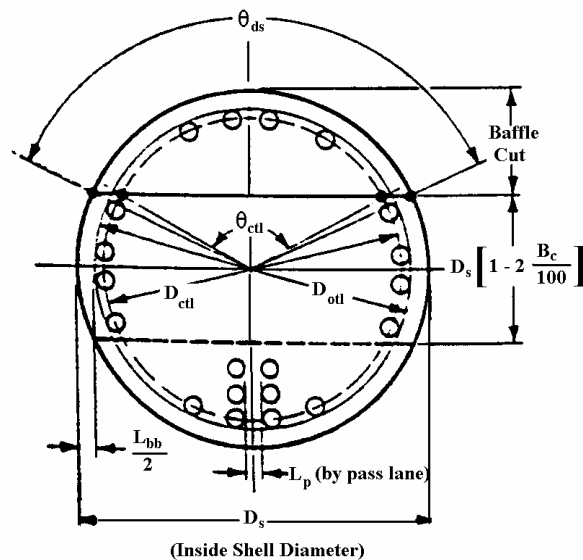


Figure 4.9 Basic baffle geometry relations

If tubes have to be omitted to accommodate impingement plates (Figure 4.8) or for reasons of shell fluid distribution, a correction factor based on subtracting from the area of the  $D_{ctl}$  circle in Eq. (4.46),  $0.78D_{ctl}^2$ , the area that is not occupied by the tubes, has to be applied. Hence, [3]

$$N_t = (N_t)_1(1 - \psi_c) \quad (4.47a)$$

where  $\psi_c$  is the correction factor calculated by the same principles as the baffle cut area shown in Figure 4.9 and Eqns. (4.62) and (4.64). Substituting the values corresponding to this situation, one gets [2, 3]

$$\theta_{ctl} = 2 \cos^{-1} \left[ \frac{D_s}{D_{ctl}} \left( 1 - 2 \frac{B_c^*}{100} \right) \right] \quad (\text{deg}) \quad (4.47b)$$

$$S_c = 0.78 D_{ctl}^2 \left( \frac{\theta_{ctl}}{360} - \frac{\sin \theta_{ctl}}{2\pi} \right) \quad (4.47c)$$

where  $S_c$  is the area of the cutoff from the  $D_{ctl}$  circle and  $B_c^*$  is the cut in percent of  $D_s$  between the inside shell diameter  $D_s$  and the cut line, similar to  $B_c$  in Figure 4.9. Then

$$B_c^* = \frac{L_{bch}^*}{D_s} 100 \quad (\%) \quad (4.47d)$$

where  $L_{bch}^*$  is the baffle cut height. The correction factor  $\psi_c$  is then

$$\psi_c = \frac{\theta_{ctl}}{360} - \frac{\sin \theta_{ctl}}{2\pi} \quad (4.47e)$$

Eq. (4.47a) is valid only for cut out on one side of the shell. If the tube field on both sides of the shell is cut in the same way (such as for no-tubes-in-window designs),  $2\psi_c$  should be used instead of  $\psi_c$ , in Eq. (4.47a).

For  $N_p > 1$  (multipass arrangement), a correction factor  $\psi_n$  must be used to account for the decrease of tube count due to tube pass

partitions.

$$N_t = (N_t)_1(1 - \psi_n) \quad (4.48)$$

The accuracy of Eq. (4.48) is approximately 10% on small shell diameters ( $D_s < 400$  mm) and 5% for larger shell diameters. [3]

- 13)  **$N_p$ , number of tube passes:** Pass partitions in a heat exchanger should be located as much as possible perpendicularly to the cross flow stream, to avoid bypass flow. If pass partitions are in the flow direction, tie rods are placed into the tube pass partitions to block the flow. For shell-side calculations,  $N_p$  is used only for estimation of tube count, as tubes are omitted on account of the pass partitions. In overall rating problems, this item is used for determination of tube-side flow velocity and for the  $\Delta T_m$  correction factor. The maximum value of  $N_p$  for a given shell diameter  $D_s$  should be observed, because otherwise too many tubes would have to be omitted from the tube field. The table showing the values of  $N_{p,max}$  according to different  $D_s$  values, is given below. [3]

$D_s$ (mm)	200	400-800	800-1200	>1200
$N_{p,max}$	2	4-6	6-8	8-10

If small tube diameters are used, large  $N_p$  numbers can be used. It should be noted that the minimum number of tubes per tube pass is approximately 8. The accuracy of the Bell-Delaware method will decrease if the above rules are violated.

- 14)  **$N_{ss}$ , number of sealing strips (pairs) in one baffle crossing:** If  $L_{bb}$ , which is the tube bundle-to-shell bypass clearance becomes large, such as in pull-through bundles, the bypass stream will reach considerable

magnitude, resulting in decreased heat transfer coefficient. To avoid this effect, ‘sealing strips’ which are usually sheet metal strips attached to the baffles, are allocated. These strips force the flow back into the tube bundle, as shown in Figure 4.10. [3] As a general rule, sealing strips should be considered if the tube bundle-to-shell diameter clearance,  $L_{bb}$ , exceeds approximately a value of 30 mm. So, all pull-through floating head designs require sealing strips whereas fixed tubesheet and U tube designs do not.

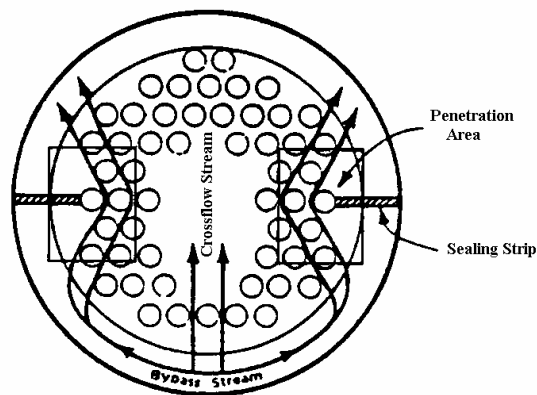


Figure 4.10 Typical flow pattern in bypass stream with sealing strip ( $N_{ss}=1$ )

- 15) **CB (code), tube bundle construction types:** The Bell-Delaware method will handle the following tube bundle types (TEMA Standards): [3, 36]
- a) U-tube bundles, code UT: UT is the least expensive construction because it needs only one tubesheet and is the best for tube expansion requirements. Only an even number of tube passes is possible. In U-tube bundles, mechanical tube-side cleaning is very difficult because of the U bend shape. The tube bundle is removable and shell-side cleaning is possible. Replacement of defective tubes cannot be made.
  - b) Fixed tube sheet, code FX: FX is the next least expensive construction, because it needs two tubesheets. However, it is

limited by tube expansion requirements (expansion bellows). Only chemical cleaning of shell-side is possible. Replacement of defective tubes is easy.

- c) Split-ring floating-head bundle, code SRFH: SRFH is used for applications where U-tube construction is not desirable but thermal expansion is required. Shell-side cleaning by mechanical means is required rarely (since complete disassembly of the rear head is necessary). More tubes per shell diameter can be accommodated than with the PTFH type; there is also much less bypass area. Replacement of defective tubes is easy.
- d) Packed floating-head bundle, code PFH: PFH is similar to SRFH except that tubesheet packing may cause problems.
- e) Pull-through floating-head bundle, code PTFH: PTFH is used when it is necessary to clean the shell-side frequently. PTFH is the easiest type for pulling the bundle for shell-side cleaning.

- 16)  **$L_{tb}$  (mm), diametral clearance between tube outside diameter  $d_o$  and baffle hole:**  $L_{tb}$  is required for determination of tube-to-baffle hole leakage stream, which is a correlational parameter of the Bell-Delaware method. TEMA Standards specify recommended clearances in the baffle tube hole as a function of tube diameter  $d_o$  and  $L_{b,max}$ , as shown in Figure 4.11. [3] Instead of TEMA Standards given in Figure 4.11, DIN Standard 28182 recommendations given below can also be used. [3]

$$L_{tb} \text{ (mm)} = \begin{cases} d_{o,max} + 0.7 - d_o \\ d_{o,max} - 0 - d_o \\ d_{o,max} + 0.4 - d_o \\ d_{o,max} - 0 - d_o \end{cases} \text{ for } L_{b,max} \begin{cases} < 1000 \text{ mm} \\ > 1000 \text{ mm} \end{cases}$$

where  $d_{o,max}$  is the maximum tube outside diameter including tolerances,

and  $d_o$  is the nominal tube outside diameter.

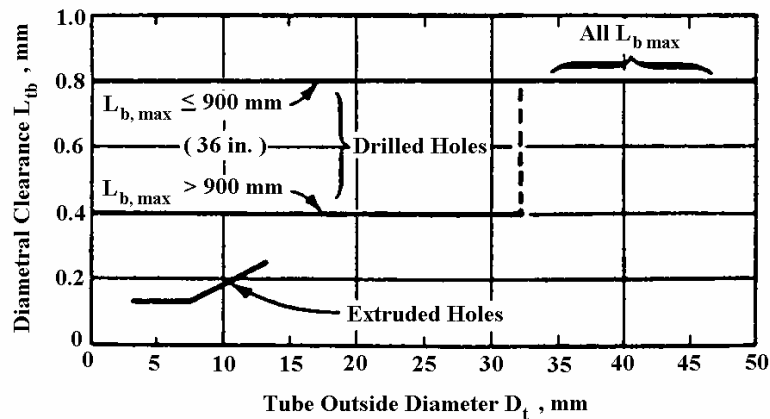


Figure 4.11 Diametral tube-to-baffle hole clearance  $L_{tb}$  as a function of tube diameter and the maximum unsupported tube length  $L_{b,max}$ , TEMA Standards and for extruded baffle holes for small-diameter shells ( $D_s < 350$  mm)

To use the above procedure, it is required to know  $d_{o,max}$ , which is very difficult to find, which depends on type of tubing material, process of manufacturing, and so on. Therefore, using Figure 4.11 is much more simpler. Figure 4.11 shows the clearance values for drilled baffle holes and for extruded baffle holes. Extruded holes are used for small shell and small diameter tubes.

- 17)  **$L_{sb}$  (mm), inside shell-to-baffle clearance (diametral):**  $L_{sb}$  is the clearance between the shell inside diameter and the baffle outside diameter. It provides a passage for the shell-to-baffle leakage stream, affecting seriously the heat transfer effectiveness. To determine the leakage area, the average diametral clearance between the shell and the baffle has to be established. The value of  $D_s$  (mm) is a nominal dimension, subject to manufacturing tolerances and out-of-roundness tolerances. The baffle outside diameter will also be subject to manufacturing tolerances. Therefore, TEMA specifies only the average

clearance  $L_{sb}$ , as a function of the shell diameter  $D_s$ . The TEMA step values are approximated with a straight line, and curve-fitted as [36]

$$L_{sb} = 1.6 + 0.004D_s \quad (\text{mm}) \quad (4.49)$$

An additional clearance of 1.5 mm is added to Eq. (4.49) because of the out-of-roundness tolerances, which are not clearly defined by TEMA. This additional clearance results in leakage areas with a greater safety factor for heat transfer but lower safety factor for pressure drop. TEMA average curve with 1.5 mm additive safety is curve-fitted as [36]

$$L_{sb} = 3.1 + 0.004D_s \quad (\text{mm}) \quad (4.50)$$

- 18)  **$L_{bb}$  (mm), inside shell diameter-to-tube bundle bypass clearance (diametral):**  $L_{bb}$  is two times the distance between the inside shell wall and the circle circumscribed to the outermost tubes of the tube field,  $D_{otl}$ , as shown in Figure 4.9. It determines the flow area for bundle bypass stream and the corresponding correction factors. The value of  $L_{bb}$  depends mainly on the tube bundle type used. U-tube and fixed tubesheet constructions require minimum clearances whereas split-ring and packed floating-head constructions require much larger clearances, to accommodate the rear head. Pull-through floating-head designs must accommodate bolts for the rear head and require still much larger clearances.

To calculate the bypass area, the tube bundle circumscribed circle,  $D_{otl}$ , is defined as [3]

$$D_{otl} = D_s - L_{bb} \quad (4.51a)$$

or

$$L_{bb} = D_s - D_{otl} \quad (4.51b)$$

The diameter of the circle through the centers of the tube located within the outermost tubes,  $D_{ctl}$ , is also required to calculate other tube field related parameters:

$$D_{ctl} = D_s - (L_{bb} + d_o) = D_{otl} - d_o \quad (4.52)$$

- 19)  **$R_{f,o}$ , (m<sup>2</sup>K/W), shell-side fouling resistance (referred to tube outside surface):** Since the fouling resistance values affect the performance of the heat exchanger, a careful consideration should be given to assigning a value to this item. It is recommended to perform also the calculations for a clean heat exchanger to see the effect of the fouling resistance assigned. If substantial fouling resistance is specified, the resulting fouling layer thickness may affect the tubular cross flow area and the tube-to-baffle hole clearances. Fouling resistance values for a variety of fluids are given in TEMA Standards in Table D.1. [36]
- 20)  **$R_{f,i}$ , (m<sup>2</sup>K/W), tube-side fouling resistance (referred to tube inside surface):** The comments given in item 19 are also valid for tube-side fouling resistance,  $R_{f,i}$ . However, even more careful consideration should be given to tube-side fouling resistance because it is a strong function of flow velocity. If tube-side fouling exists on externally low-finned tubes, this resistance will be multiplied by the ratio of outside to inside tube surface which is approximately 3, if the overall heat transfer coefficient is based on the outside tube surface area. [3]
- 21)  **$\Delta p_{s,max}$ ,  $\Delta p_{t,max}$ , maximum permissible pressure drops for shell-side and tube-side, respectively:** The best utilization of the allowed  $\Delta p$  given in the design problem will result in the least expensive and most efficient heat exchanger.

- 22)  $v_{t,max}$  (m/s), **maximum allowable tube-side flow velocity**: In design problems, the maximum permissible tube-side flow velocity is specified sometimes instead of and/or in addition to the maximum permissible pressure drop. This is due to the erosion effects related to tube material used and the nature of the tube-side fluid (clean or with abrasive particles present). A very rough estimation of  $v_{t,max}$  for clean fluids is 3 m/s for carbon steel or Cu-Ni alloys, 5 m/s for alloyed steels, and 6 m/s for titanium tubes. The presence of abrasive particles will require the lowering of these limits, especially in U tubes. [3]
- 23)  $v_{t,min}$  (m/s), **minimum allowable tube-side flow velocity**: The rate of fouling for most fluids is strongly dependent on the flow velocity. Therefore, a minimum tube-side velocity is required to prevent flow velocity-sensitive fouling. Consequently, the heat exchanger designer has to respect this limitation and eliminate design configurations that appear otherwise acceptable but that do not meet this restriction. For liquids in turbulent flow,  $v_{t,min}$  should not be below about 1.0 m/s and preferably more; for cooling water,  $v_{t,min}$  should be 1.0 m/s, but a generally accepted value in design is  $v_t \approx 2$  m/s considering the overall cost optimizations between pumping power cost and cost of fouling. [3]

The other input data used in the Bell-Delaware method such as shell-side inlet temperature,  $T_{s,i}$ , shell-side outlet temperature,  $T_{s,o}$ , tube-side inlet temperature,  $T_{t,i}$ , tube-side outlet temperature,  $T_{t,o}$ , shell-side fluid mass flow rate,  $\dot{m}_s$ , tube-side fluid mass flow rate,  $\dot{m}_t$ , density at shell-side fluid mean temperature,  $\rho_s$ , density at tube-side fluid mean temperature,  $\rho_t$ , thermal conductivity at shell-side fluid mean temperature,  $k_s$ , thermal conductivity at tube-side fluid mean temperature,  $k_t$ , specific heat at shell-side fluid mean temperature,  $(c_p)_s$ , specific heat at tube-side fluid mean temperature,  $(c_p)_t$ ,

dynamic viscosity at shell-side fluid mean temperature,  $\mu_s$ , and, dynamic viscosity at tube-side fluid mean temperature,  $\mu_t$ , are all self-explanatory. [2, 3]

#### 4.3.4 Calculations of Bell-Delaware Method

##### 1) Cross flow area $S_m$ at the shell centerline with one baffle spacing $B$

This is the minimum cross flow area in the shell-side flow direction (perpendicular to the baffle cut). This area has two components. One of them is the bypass channel between the tube bundle and shell inside diameter,  $L_{bb}$ . The other component is the minimum cross-sectional area within the tube field. As can be seen from Table 4.1, for 30° and 90° layouts, the minimum free cross flow gap is simply  $(P_T - d_o)$  for each tube pitch  $P_T$  and for the 45° staggered layout, the minimum cross flow gap within the layout pattern is the sum of the two gaps in the triangle sides  $(P_T - d_o)$ . Therefore, [2, 3]

$$S_m = B \left[ L_{bb} + \frac{D_{ctl}}{P_{T,eff}} (P_T - d_o) \right] \quad (4.53)$$

where  $B$  is the central baffle spacing,  $L_{bb}$  is the bypass channel diametral gap, and  $P_{T,eff}$  is a new term which normalizes the calculational procedures. [3] Note that

$$P_{T,eff} = P_T \quad \text{for } 30^\circ \text{ and } 90^\circ \text{ layouts}$$

$$P_{T,eff} = 0.707P_T \quad \text{for } 45^\circ \text{ staggered layout}$$

As a result, the 45° layout will have 1.41 times larger cross flow area (based on tube pitch  $P_T$ ) than either the 90° or the 30° layout, but the number of tube rows crossed will be 1.41 and 1.22 larger than in the 90° and 30° layouts, respectively.

**2) Average temperatures,  $T_{s,av}$  ,  $T_{t,av}$**

The physical properties in calculations of Bell-Delaware method are evaluated at the arithmetic mean temperatures of the shell and tube-side fluids:

$$T_{s,av} = \frac{1}{2}(T_{s,i} + T_{s,o}) \quad (4.54a)$$

$$T_{t,av} = \frac{1}{2}(T_{t,i} + T_{t,o}) \quad (4.54b)$$

**3) Shell-Side Reynolds number,  $Re_s$**

The maximum shell-side cross flow mass velocity,  $G_s$  is defined as [2, 3, 4]

$$G_s = \frac{\dot{m}_s}{S_m} \quad (4.55)$$

where  $\dot{m}_s$  is the shell-side flow rate, and  $S_m$  is the cross flow area determined from Eq. (4.53). The shell-side Reynolds number  $Re_s$  is then calculated from [2, 3, 4]

$$Re_s = \frac{d_o G_s}{\mu_s} \quad (4.56)$$

where  $d_o$  is the tube outside diameter,  $\mu_s$  is the dynamic viscosity at average bulk temperature, and  $G_s$  is the shell-side mass velocity defined by Eq. (4.55).

#### 4) Shell-Side Prandtl Number, $Pr_s$

Shell-side Prandtl number can be calculated from

$$Pr_s = \frac{c_{p,s} \mu_s}{k_s} \quad (4.57)$$

where  $c_{p,s}$  is the shell-side fluid specific heat,  $\mu_s$  is the shell-side fluid dynamic viscosity, and  $k_s$  is the shell-side fluid thermal conductivity. The physical properties  $c_{p,s}$ ,  $\mu_s$ , and  $k_s$  are all taken at the average shell fluid temperature.

#### 5) Mean temperature difference, $\Delta T_m$

The effective mean temperature difference is discussed in detail in Section 3.4. From basic definitions,

$$\Delta T_m = \Delta T_{lm} (F) \quad (4.58)$$

where  $F$  is the correction factor calculated for any particular flow configuration as determined in Section 3.4., and  $\Delta T_{lm}$  is the log-mean temperature difference for counter flow given by Eq. (3.19) where  $\Delta T_1$  and  $\Delta T_2$  are the terminal temperature differences of the hot and cold streams as explained in Section 3.4.

#### 6) Total heat transfer surface of the exchanger, $A_o$

The heat transfer effective tubular area, pertaining to the effective tube length  $L_{ta}$ , is expressed as [3, 4]

$$A_o = \pi d_o L_{ta} N_t \quad (4.59)$$

## 7) Segmental baffle window calculations

Figure 4.9 illustrates the basic baffle geometry relations. The centri-angle of the baffle cut intersection with the inside shell wall,  $\theta_{ds}$  can be calculated from [3]

$$\theta_{ds} = 2 \cos^{-1} \left[ 1 - 2 \left( \frac{B_c}{100} \right) \right] \quad (\text{deg}) \quad (4.60)$$

The angle intersecting the diameter  $D_{ctl}$ , that is, the circle through the centers of the outermost tubes, is expressed as [3]

$$\theta_{ctl} = 2 \cos^{-1} \left\{ \frac{D_s}{D_{ctl}} \left[ 1 - 2 \left( \frac{B_c}{100} \right) \right] \right\} \quad (\text{deg}) \quad (4.61)$$

If window baffles where the area between  $D_s$  and  $D_{otl}$  is blocked, the centri-angle referred to  $D_{otl}$  is needed: [3]

$$\theta_{otl} = 2 \cos^{-1} \left\{ \frac{D_s}{D_{otl}} \left[ 1 - 2 \left( \frac{B_c}{100} \right) \right] \right\} \quad (\text{deg}) \quad (4.62)$$

## 8) Baffle window flow areas

The gross window flow area, that is, without tubes in the window,  $S_{wg}$ , is [2, 3]

$$S_{wg} = \frac{\pi}{4} (D_s)^2 \left( \frac{\theta_{ds}}{360} - \frac{\sin \theta_{ds}}{2\pi} \right) \quad (4.63)$$

The results of Eq. (4.63) are also plotted in graphical form [3] as a function of  $D_s$ , with  $B_c$  as a parameter.

Assuming that the tube field is uniform (neglecting the tube pass lanes) within the diameter  $D_{otl}$ , the fraction of number of tubes in one baffle window,  $F_w$  is expressed as [3]

$$F_w = \frac{\theta_{ctl}}{360} - \frac{\sin \theta_{ctl}}{2\pi} \quad (4.64)$$

where  $\theta_{ctl}$  is defined by Eq. (4.61). The fraction of number of tubes in pure cross flow between the baffle cut tips,  $F_c$  is expressed as

$$F_c = 1 - 2(F_w) \quad (4.65)$$

The segmental baffle window area occupied by the tubes,  $S_{wt}$ , is calculated as [3]

$$S_{wt} = N_t F_w \left( \frac{\pi}{4} d_o^2 \right) = N_{tw} \left( \frac{\pi}{4} d_o^2 \right) \quad (4.66)$$

where  $N_{tw}$  is the number of tubes in the window and is expressed as

$$N_{tw} = N_t F_w \quad (4.67)$$

Therefore, the net cross flow area through one baffle window,  $S_w$ , that is the gross flow area  $S_{wg}$ , Eq. (4.63), minus the area occupied by the tubes,  $S_{wt}$ , Eq. (4.66), is

$$S_w = S_{wg} - S_{wt} \quad (4.68)$$

## 9) Equivalent hydraulic diameter of a segmental baffle window, $D_w$

The equivalent hydraulic diameter of a segmental baffle window,  $D_w$ , is

required only for pressure drop calculations in laminar flow. It is four times the window cross flow area  $S_w$  divided by the periphery length in contact with the flow. This is given by the following equation: [3]

$$D_w = \frac{4S_w}{\pi d_o N_{tw} + \pi D_s \theta_{ds} / 360} \quad (4.69)$$

**10) Number of effective tube rows in cross flow,  $N_{tcc}$  and  $N_{tcw}$**

The number of tubes in cross flow is required for the calculation of heat transfer coefficient and pressure drop, and the corresponding correction factors. It is a function of the tube layout and tube pitch. The number of effective rows crossed in one cross flow section, that is, between the baffle tips, is [1, 2, 3]

$$N_{tcc} = \frac{D_s}{P_p} \left[ 1 - 2 \left( \frac{B_c}{100} \right) \right] \quad (4.70)$$

where  $P_p$  is obtained from Table 4.1. The determination of the number of effective tube rows crossed in the baffle window,  $N_{tcw}$ , is not straightforward and is subject to some interpretation of the window flow pattern. Highest flow velocity exists just below the baffle tips and then decreases rapidly. This was demonstrated by numerous visual experiments. So, the effective distance of baffle window flow penetration, which could be considered cross flow, must be determined from experimental data. From the Delaware and other data, the effective distance of penetration,  $L_{wp}$ , was determined as 0.4 of the tubular field in the baffle window, which is the distance between the baffle cut and  $D_{ctl}$ . [3]

$$L_{wp} = 0.4 \left( D_s \left( \frac{B_c}{100} \right) - \frac{D_s - D_{ctl}}{2} \right) \quad (4.71)$$

This distance is crossed twice within each window, and therefore the effective number of tube rows crossed,  $N_{icw}$ , is

$$N_{icw} = \frac{0.8}{P_p} \left[ D_s \left( \frac{B_c}{100} \right) - \frac{D_s - D_{ctl}}{2} \right] \quad (4.72)$$

where  $P_p$  is the effective tube row distance in the flow direction and is given in Table 4.1. [3]

#### 11) Number of baffles, $N_b$

In the calculation of the total number of cross passes and window turnarounds, the number of baffles  $N_b$  is needed. If  $N_b$  has to be calculated, the summation of all baffle spacings  $L_{ti}$  and the baffle spacing  $B$  are used: [2, 3]

$$N_b = \frac{L_{ti}}{B} - 1 \quad (4.73)$$

#### 12) Bundle-to-shell bypass area parameters, $S_b$ and $F_{sbp}$

The prime area where the flow can bypass the desirable path through the tube field is the flow area between the shell wall and the tube bundle. The flow in the bypass area has a lower resistance than that through the bundle and therefore decreases the efficiency of heat transfer while decreasing the pressure drop. In addition to the shell-to-bundle bypass area, there can be additional bypass flow in tube partition pass lanes. Accordingly, the bypass area within one baffle,  $S_b$ , can be expressed as follows: [2, 3]

$$S_b = B \left[ (D_s - D_{otl}) + L_{pl} \right] \quad (4.74)$$

where  $L_{pl}$  expresses the effect of the tube lane partition bypass width (between tube walls) as shown in Figure 4.9.  $L_{pl}$  is taken as zero for all standard

calculations or as half of the real dimension of the tube lane partition  $L_p$ . For estimation purposes assume that  $L_p = d_o$ .

For the calculations of the correction factors  $J_b$  and  $R_b$ , the fraction of the bypass area  $S_b$  to the overall cross flow area  $S_m$ , is needed: [2, 3]

$$F_{sbp} = \frac{S_b}{S_m} \quad (4.75)$$

### 13) Shell-to-baffle leakage area, $S_{sb}$

The shell-to-baffle leakage area  $S_{sb}$  is required for calculation of the correction factors for baffle leakage effects  $J_l$  and  $R_l$ . The shell-to-baffle leakage area within the circle segment occupied by the baffle is calculated (with acceptable approximation) as [2, 3]

$$\begin{aligned} S_{sb} &= \pi D_s \left( \frac{L_{sb}}{2} \right) \left( \frac{360 - \theta_{ds}}{360} \right) \\ &= 0.00436 D_s L_{sb} (360 - \theta_{ds}) \end{aligned} \quad (4.76)$$

where  $L_{sb}$  is the diametral leakage clearance between the shell diameter  $D_s$  and the baffle diameter  $D_b$ .

### 14) Tube-to-baffle hole leakage area for one baffle, $S_{tb}$

The tube-to-baffle hole leakage area for one baffle,  $S_{tb}$ , is needed for calculation of the correction factors  $J_l$  and  $R_l$ . The diametral clearance  $L_{tb}$  is a data input item with recommended values shown in Figure 4.11. The total tube-to-baffle leakage area within one baffle is then [2, 3]

$$S_{tb} = \left\{ \frac{\pi}{4} [(d_o + L_{tb})^2 - d_o^2] \right\} (N_t)(1 - F_w) \quad (4.77)$$

where  $F_w$  is related to  $F_c$ , the fraction of tubes in the baffle between baffle tips, as calculated in Eq. (4.65). The expression in braces in this equation represents the leakage area for one tube  $(S_{tb})_1$ . Therefore, Eq. (4.77) can be rewritten as

$$S_{tb} = (S_{tb})_1 (N_t)(1 - F_w) \quad (4.78)$$

### 15) Segmental baffle window correction factor $J_c$

The correction factor  $J_c$  is used to express the effects of the baffle window flow on the heat transfer factor  $j$ , which is based on cross flow. Postulating a number of logical assumptions on how the window flow is related to the cross flow at shell centerline, the Delaware workers developed this correction factor. The method is very simple and reasonable for the range of recommended baffle cuts and baffle spacing values.  $J_c$  reaches the value of 1.0 for baffle cuts around 25 to 30%, and even larger than 1.0 for smaller baffle cuts because  $j_i$  is obtained at the largest cross flow section at the center row, while much higher flow velocities will exist below the baffle cut edge, especially as the baffle cut decreases. This is compensated by the fact that fewer tubes exist in this region. [2, 3, 40]

The factor  $J_c$  is a function of the baffle cut  $B_c$  and of the diameter  $D_{cl}$  since both values determine the number of tubes in the baffle window. The correlating parameter is the fraction of tubes in cross flow (between baffle tips), given as  $F_c$  in Eq. (4.65).  $J_c$  is expressed as [3]

$$J_c = 0.55 + 0.72F_c \quad (4.79)$$

## 16) Correction factors for baffle leakage effects for heat transfer, $J_1$ , and pressure drop, $R_1$

The pressure difference between two adjoining baffle compartments forces part of the flow to penetrate in the gap between (a) the shell and the baffle edge circumference (b) the tube and the baffle tube holes. This decreases the effective cross flow stream and consequently both the actual shell-side heat transfer coefficient and the shell-side pressure drop. The leakage streams can reach considerable magnitudes (up to 40%) and are, therefore, most important factors in the correlations. From the two leakage streams considered, the shell-to-baffle stream is most detrimental to heat transfer because it does not exchange heat with any tubes. However, since the tube-to-baffle stream passes over the tube surface within the gap, it is only partially effective. But note that the tube hole clearances may become plugged up by fouling deposits in some cases, and consequently this stream may decrease with time. This will increase the cross flow stream but also the other bypass streams, with the usual effect of a relatively small change of heat transfer but usually increased pressure drop. [3, 39, 40]

One of the correlational parameters used in the calculation of  $J_1$  and  $R_1$ , is [2, 3]

$$r_{lm} = \frac{S_{sb} + S_{tb}}{S_m} \quad (4.80)$$

which is the ratio of both leakage areas to the cross flow area. In Eq. (4.80),  $S_{sb}$  is the shell-to-baffle leakage area calculated by Eq. (4.76),  $S_{tb}$  is the tube-to-baffle hole leakage area calculated by Eq. (4.78), and  $S_m$  is the cross flow area at the bundle centerline determined by Eq. (4.53). The other parameter is the ratio of the shell-to-baffle leakage area to the sum of both leakage areas and is expressed as follows: [2, 3]

$$r_s = \frac{S_{sb}}{S_{sb} + S_{tb}} \quad (4.81)$$

The most severe correction is for the parameter  $r_s = 1$ , which corresponds to the case of all leakage taking place in the shell-to-baffle area. The least severe correction is for the case of all leakage in the tube baffle holes,  $r_s = 0$ . A well-designed exchanger should have values of  $J_l$  not less than about 0.6, preferably 0.7-0.9, because otherwise too great penalty on heat transfer efficiency will exist.

For computer applications, the correction factors are curve-fitted as follows:

$$J_l = 0.44(1 - r_s) + [1 - 0.44(1 - r_s)] \exp(-2.2r_{im}) \quad (4.82a)$$

$$R_l = \exp\left\{-1.33(1 + r_s)(r_{im})^p\right\} \quad (4.82b)$$

where  $p = [-0.15(1 + r_s) + 0.8]$ . These correction factors are also shown in graphical forms as a function of  $r_{im}$  for various values of  $r_s$ . [2, 3, 39, 40]

### 17) Correction factors for bundle bypass effects for heat transfer, $J_b$ , and pressure drop, $R_b$

The flow resistance in the shell-to-bundle bypass is substantially lower than through the tube field. Consequently, part of the flow will seek this path, in proportion to the ratio of the resistances of the bypass area to the tube field cross flow area. Since this stream touches the tubes on one side, it is only partially effective for heat transfer. For fixed-tube sheet and U-tube bundles, the bypass area is usually not too large. However, for pull-through bundles, the bypass channel must be blocked by sealing strips.

One of the parameters used in the calculation of  $J_b$  and  $R_b$  is  $F_{sbp}$ , which is the ratio of bypass to cross flow area given in Eq. (4.75). If sealing strips are used,  $N_{ss}$ , which is the number of sealing strips (pairs) in one baffle, and,  $N_{tcc}$ , which is the number of tube rows crossed between baffle tips in one baffle

section, given in Eq. (4.70), must also be known and hence  $r_{ss}$  which is given as [3]

$$r_{ss} = \frac{N_{ss}}{N_{icc}} \quad (4.83)$$

must be determined.

For computer applications, the correction factors are curve-fitted as follows: [2, 3]

$$J_b = \exp \left\{ -C_{bh} F_{sbp} \left( 1 - \sqrt[3]{2r_{ss}} \right) \right\} \quad (4.84)$$

with the limit of  $J_b = 1$ , at  $r_{ss} \geq \frac{1}{2}$ , and  $C_{bh} = 1.35$  for laminar flow,  $Re_s \leq 100$ ,  $C_{bh} = 1.25$  for turbulent and transition flow,  $Re_s > 100$ , and

$$R_b = \exp \left\{ -C_{bp} F_{sbp} \left( 1 - \sqrt[3]{2r_{ss}} \right) \right\} \quad (4.85)$$

with the limit of  $R_b = 1$ , at  $r_{ss} \geq \frac{1}{2}$ , and  $C_{bp} = 4.5$  for laminar flow,  $Re_s \leq 100$ ,  $C_{bp} = 3.7$  for turbulent and transition flow,  $Re_s > 100$ . [2, 3]

The correction factors for heat transfer  $J_b$  and for pressure drop  $R_b$  are also shown in graphical forms. [2, 3, 39, 40]

### 18) Heat transfer correction factor for adverse temperature gradient in laminar flow, $J_r$

The Delaware data for  $Re_s \lesssim 20$  exhibited a large decrease of heat transfer. Above  $Re > 20$ , momentum change or inertial effects begin to disturb the laminar layer buildup and the effect decreases, until at approximately  $Re = 100$ , it disappears. [2]

Since the ideal tube bank  $j_i$  curves are based on 10 tube rows, the corresponding factor  $J_r$  for  $Re_s \leq 20$  can be expressed as [3]

$$J_r = (J_r)_r = \left( \frac{10}{N_c} \right)^{0.18} = \frac{1.51}{(N_c)^{0.18}} \quad (4.86)$$

where  $N_c$  is the total number of tube rows crossed in the entire heat exchanger:

$$N_c = (N_{icc} + N_{icw})(N_b + 1) \quad (4.87)$$

Between  $Re_s \leq 20$  and  $Re_s = 100$ , the heat transfer correction factor  $J_r$  can be expressed as [3]

$$J_r = (J_r)_r + \left( \frac{20 - Re_s}{80} \right) [(J_r)_r - 1] \quad (4.88)$$

where  $(J_r)_r$  is calculated from Eq. (4.86) with the limits: [2, 3]

$$\begin{aligned} J_r &= 1 && \text{for } Re_s > 100 \\ J_r &= (J_r)_r && \text{for } Re_s \leq 20 \ ; \ J_r \geq 0.4 \end{aligned}$$

The correction factor  $J_r$  is also shown in graphical form. [2, 3, 39, 40]

### 19) Heat transfer correction for unequal baffle spacing at inlet and/or outlet, $J_s$

Refer to Figure 4.7 which shows a schematic sketch of an exchanger where the inlet and outlet baffle spacing  $B_i$  and  $B_o$  are enlarged in comparison to the regular central spacing  $B$ . Assume that the heat transfer coefficient  $h_i$  is calculated on the basis of the central spacing  $B$  and that  $h_i$  is proportional to

$v_{\max}^n$ , where  $v_{\max}$  is the cross flow velocity based on  $B$ . Here  $n$  is approximately a constant, assumed to be 0.6 for turbulent flow and 1/3 for laminar flow. Assuming that the leakage and bypass flow ratios are not greatly changed by the difference between  $B$  and  $B_i$  or  $B_o$  (which should be the case for well-designed exchangers where the case of  $B_i$  too much greater than  $B$  is not acceptable), then [3]

$$h_i \propto v_{\max}^n \propto \left(\frac{1}{B}\right)^n \quad (4.89)$$

The mean shell-side heat transfer coefficient  $h_s$ , which takes into account the different coefficients in the inlet and outlet spacing  $(h_i)_i$  and  $(h_i)_o$ , coupled to the respective heat transfer areas  $(A_o)_i$  and  $(A_o)_o$  is written as [3]

$$h_s A_o = (h_i)_i (A_o)_i + h_i [A_o - (A_o)_i - (A_o)_o] + (h_i)_o (A_o)_o \quad (4.90)$$

The correction factor  $J_s$  can now be defined as a multiplier to the  $h_i$  value by dividing Eq. (4.90) by the product of  $h_i A_o$ . [3]

$$J_s = \frac{h_s}{h_i} = \frac{(h_i)_i}{h_i} \left[ \frac{(A_o)_i}{A_o} \right] + \frac{A_o - (A_o)_i - (A_o)_o}{A_o} + \frac{(h_i)_o}{h_i} \left[ \frac{(A_o)_o}{A_o} \right] \quad (4.91)$$

Introducing the following relationships [3]

$$\frac{h_i}{(h_i)_i} = \left(\frac{B_i}{B}\right)^n = (L_i^*)^n \quad (4.92)$$

$$\frac{h_i}{(h_i)_o} = \left(\frac{B_o}{B}\right)^n = (L_o^*)^n \quad (4.93)$$

where  $L_o^*$  and  $L_i^*$  are dimensionless length ratios, it is noted that

$$\frac{A_o - (A_o)_i - (A_o)_o}{A_o} = \frac{N_b - 1}{L_i^* + (N_b - 1) + L_o^*} \quad (4.94)$$

Then Eq. (4.91) becomes [2, 3]

$$J_s = \frac{(N_b - 1) + (L_i^*)^{(1-n)} + (L_o^*)^{(1-n)}}{(N_b - 1) + L_i^* + L_o^*} \quad (4.95)$$

$J_s = 1.0$  for  $B_i = B_o = B$  or  $L^* = L_i^* = L_o^* = 1.0$ .  $J_s$  is also shown in graphical form [2, 3, 39, 40] as a function of number of baffles  $N_b$  for various values of  $L^*$  which is written as

$$L^* = \frac{B_o}{B} = \frac{B_i}{B_o} \quad (4.96)$$

If  $L^*$  is larger than 2, it would be considered poor design, especially if combined with low  $N_b$ . In such cases an annular distributor or other measures should be used.

For laminar flow, the correction factor  $J_s$  is about halfway between 1 and  $J_s$  computed for turbulent conditions. [3]

## 20) Pressure drop correction for unequal baffle spacing at inlet and/or outlet, $R_s$

From equations of pressure drop, [3]

$$\Delta p_{bi} \propto \left( \frac{1}{B} \right)^{2-n} \quad (4.97)$$

where  $\Delta p_{bi}$  is the pressure drop in cross flow between baffle tips, based on ideal

tube bank,  $n$  is the slope of the friction factor curve, assuming that  $n = 1$  for laminar flow, ( $Re_s < 100$ ), and  $n \approx 0.2$  for turbulent flow. Because of the specific way pressure drop is treated in this method as shown in Figures 4.12, 4.13 and 4.14 [2, 3, 4], a simple geometric analogy gives [3]

$$R_s = \left(\frac{B}{B_o}\right)^{2-n} + \left(\frac{B}{B_i}\right)^{2-n} \quad (4.98)$$

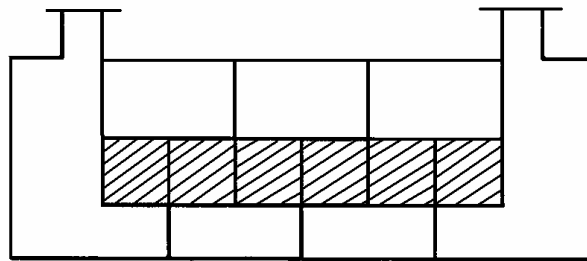


Figure 4.12 Region of cross flow between baffle tips in the central baffle spacing

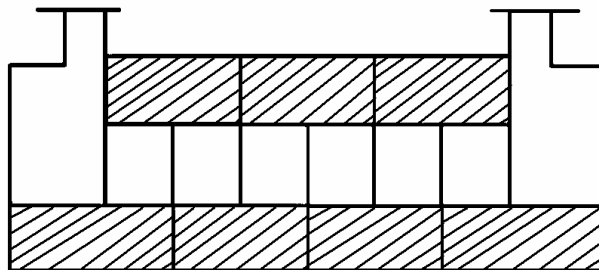


Figure 4.13 Flow region considered for window flow

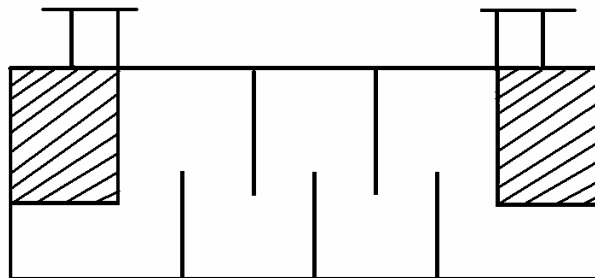


Figure 4.14 Flow region for the end baffle spacings

This development assumes that the flow regime (exponent  $n$ ) is the same throughout the exchanger. The correction factor  $R_s$  has the following characteristics: [3]

- (a) For  $B = B_o = B_i$ ,  $R_s = 2$ .
- (b) For the reasonably extreme case  $B_o = B_i = 2B$ ,  $R_s = 1.0$  for laminar flow and  $R_s = 0.57$  for turbulent flow.
- (c) For a typical U tube,  $B_i = B$  and  $B_o = 2B$ ,  $R_s = 1.5$  for laminar flow, and  $R_s = 1.3$  for turbulent flow.

#### 4.3.5 Calculation of Shell-Side Heat Transfer Coefficient and Pressure Drop

##### 1) Shell-side heat transfer coefficient, $h_s$

Using the correction factors for nonidealities of baffled flow, the actual shell-side heat transfer coefficient  $h_s$  is expressed as [2, 3, 4, 40]

$$h_s = h_i (J_c J_l J_b J_s J_r) \quad (4.99)$$

where  $h_i$  is the heat transfer coefficient for pure cross flow in ideal tube bank,  $J_c$  is the segmental baffle window correction factor, Eq. (4.79),  $J_l$  is the baffle leakage correction factor, Eq. (4.82),  $J_b$  is the bypass correction factor, tube bundle to shell, Eq. (4.84),  $J_s$  is the unequal inlet/outlet baffle spacing correction factor, applicable only if such differences exist, Eq. (4.95), and  $J_r$  is the laminar heat transfer correction factor, applicable for  $Re_s < 100$ , Eq. (4.88). These correction factors may be particularly important for U-tube bundles, where larger outlet baffle spacing will always exist unless special provisions are made, such as if the outlet nozzle is located so that the U-bend area is ineffective, which is the safe procedure. Otherwise, it is assumed that  $B_o = 1.2D_s$  for calculation of  $J_s$ , because of the large bypass areas, which have not been accounted for in the

calculation of  $h_i$ . To see the overall effectiveness of the baffled exchanger as compared to ideal tube bank, it is considered useful to calculate  $J_{tot}$ , Eq. (4.99), as the product of all the correction factors. In general,  $J_{tot}$  should never be less than 0.4, and preferably  $\geq 0.5$  for a good design.

The ideal tube bank-based coefficient  $h_i$  in Eq. (4.99) is calculated from [3]

$$h_i = j_i (c_p)_s \left( \frac{\dot{m}_s}{A_s} \right) \left( \frac{k_s}{(c_p)_s \mu_s} \right)^{2/3} \left( \frac{\mu_s}{\mu_{s,w}} \right)^{0.14} \quad (4.100)$$

where  $(c_p)_s$  is the specific heat for the shell-side fluid,  $\dot{m}_s$  is the flow rate of the shell-side fluid,  $A_s$  is the cross flow area at the centerline of the shell for one cross flow between two baffles given by Eq. (4.18),  $k_s$  is the thermal conductivity for shell-side fluid,  $\mu_s$  is the viscosity of the shell-side fluid,  $\mu_{s,w}$  is the viscosity of the shell-side fluid at the wall layer, and  $j_i$  is the Colburn  $j$ -factor for an ideal tube bank.

$j_i$  and  $f_i$  are also given in graphical forms for ideal tube bank as a function of shell-side Reynolds number,  $Re_s = d_o \dot{m}_s / \mu_o A_s$ ; tube layout; and pitch size. [3, 4]  $A_s$  is given by Eq. (4.18), that is, the Reynolds number is based on the outside tube diameter and on the minimum cross-section flow area at the shell diameter. Friction coefficients for ideal tube banks are also given on the same graphs for the pressure drop calculations.

For computer applications, the ideal values of  $j_i$  and  $f_i$  are curve-fitted as follows: [3]

$$j_i = a_1 \left( \frac{1.33}{P_T/d_o} \right)^a (Re_s)^{a_2} \quad (4.101)$$

where

$$a = \frac{a_3}{1 + 0.14(\text{Re}_s)^{a_4}}$$

and

$$f_i = b_1 \left( \frac{1.33}{P_T/d_o} \right)^b (\text{Re}_s)^{b_2} \quad (4.102)$$

where

$$b = \frac{b_3}{1 + 0.14(\text{Re}_s)^{b_4}}$$

$a_1, a_2, a_3, a_4, b_1, b_2, b_3$  and  $b_4$  are correlation coefficients listed in Table 4.2. [3, 4]

Table 4.2 Correlation coefficients for  $j_i$  and  $f_i$

Layout Angle	Reynolds Number	$a_1$	$a_2$	$a_3$	$a_4$	$b_1$	$b_2$	$b_3$	$b_4$
30°	10 <sup>5</sup> -10 <sup>4</sup>	0.321	-0.388	1.450	0.519	0.372	-0.123	7.00	0.500
	10 <sup>4</sup> -10 <sup>3</sup>	0.321	-0.388			0.486	-0.152		
	10 <sup>3</sup> -10 <sup>2</sup>	0.593	-0.477			4.570	-0.476		
	10 <sup>2</sup> -10	1.360	-0.657			45.100	-0.973		
	<10	1.400	-0.667			48.000	-1.000		
45°	10 <sup>5</sup> -10 <sup>4</sup>	0.370	-0.396	1.930	0.500	0.303	-0.126	6.59	0.520
	10 <sup>4</sup> -10 <sup>3</sup>	0.370	-0.396			0.333	-0.136		
	10 <sup>3</sup> -10 <sup>2</sup>	0.730	-0.500			3.500	-0.476		
	10 <sup>2</sup> -10	0.498	-0.656			26.200	-0.913		
	<10	1.550	-0.667			32.00	-1.000		
90°	10 <sup>5</sup> -10 <sup>4</sup>	0.370	-0.395	1.187	0.370	0.391	-0.148	6.30	0.378
	10 <sup>4</sup> -10 <sup>3</sup>	0.107	-0.266			0.0815	+0.022		
	10 <sup>3</sup> -10 <sup>2</sup>	0.408	-0.460			6.0900	-0.602		
	10 <sup>2</sup> -10	0.900	-0.631			32.1000	-0.963		
	<10	0.970	-0.667			35.0000	-1.000		

## 2) Shell-side pressure drop, $\Delta p_s$

For a shell-and-tube type heat exchanger with bypass and leakage streams, the total nozzle-to-nozzle pressure drop is calculated as the sum of the following

three components:

1. By considering the pressure drop in the interior cross flow section (baffle tip to baffle tip), the combined pressure drop of all the interior cross flow section is [2, 3, 4]

$$\Delta p_c = \Delta p_{bi}(N_b - 1)R_l R_b \quad (4.103)$$

where  $N_b$  is the number of baffles,  $R_l$  is the leakage correction factor (A and E streams) from Eq. (4.82b),  $R_b$  is the bypass correction factor from Eq. (4.85). Typically,  $R_b = 0.5$  to  $0.8$ , depending on the construction type and number of sealing strips, and  $R_l = 0.4$  to  $0.5$ . The section of the exchanger covered by this pressure drop component is shown in Figure 4.12.  $\Delta p_{bi}$  in Eq. (4.103) is the pressure drop in an equivalent ideal tube bank in one baffle compartment of central baffle spacing and it is calculated from [3]

$$\Delta p_{bi} = 4f_i \frac{G_s^2}{2\rho_s} \left( \frac{\mu_{s,w}}{\mu_s} \right)^{0.14} N_{tcc} \quad (4.104)$$

where  $f_i$  is the friction coefficient given by Eq. (4.102),  $G_s$  is the mass velocity of the shell-side fluid,  $\rho_s$  is the shell-side fluid density,  $\mu_s$  is the shell-side fluid viscosity,  $\mu_{s,w}$  is the viscosity of shell-side fluid evaluated at wall surface temperature, and  $N_{tcc}$  is the number of tube rows crossed in one cross flow section, that is, between the baffle tips.

2. The pressure drop in the window is affected by leakage but not bypass. The combined pressure drop  $\Delta p_w$  in all the windows crossed, which equals  $N_b$ , is shown in Figure 4.13. The Delaware method offers two different correlations for  $\Delta p_w$ , one for turbulent flow and one for laminar flow, based for simplicity on the shell-side cross flow  $Re_s$ . Both correlations employ for mass velocity

calculations, the geometric mean of the cross flow area  $S_m$  given by Eq. (4.53) and the window net area  $S_w$  given by Eq. (4.68). [3]

$$\dot{m}_w = \frac{\dot{m}_s}{\sqrt{S_m S_w}} \quad (4.105)$$

where  $\dot{m}_s$  is the mass flow rate of the shell-side fluid, and  $\dot{m}_w$  is the shell-side flow mass velocity through segmental baffle window. The baffle window  $\Delta p_w$  is defined as follows:

For turbulent flow,  $Re_s \geq 100$ ,  $\Delta p_w$  is [3, 4]

$$\Delta p_w = N_b \left[ (2 + 0.6 N_{icw}) \frac{(\dot{m}_w^2)}{2 \rho_s} (10^{-3}) \right] R_l \quad (4.106)$$

The factor 2 accounts for velocity heads due to the window turnaround, and 0.6 accounts for the cross flow frictional effects over  $N_{icw}$  which is the number of tube rows crossed in the window, given by Eq. (4.72).

For laminar flow,  $Re_s < 100$ ,  $\Delta p_w$  is [3, 4]

$$\Delta p_w = N_b \left\{ 26 \frac{(\dot{m}_w)(c_p)_s}{\rho_s} \left[ \frac{N_{icw}}{L_{tp} - d_o} + \frac{B}{(D_w)^2} \right] + \left[ 2(10^{-3}) \frac{(\dot{m}_w)^2}{2 \rho_s} \right] \right\} R_l \quad (4.107)$$

where  $D_w$  is the hydraulic diameter of the baffle window defined in Eq. (4.69). The first term in brackets accounts for the cross flow and longitudinal friction, respectively; the second term in brackets represents two velocity heads for the turnaround in the window. It should be noted that only the leakage correction factor  $R_l$  is applied to the baffle window  $\Delta p_w$ , whereas the bypass correction factor  $R_b$  is considered not applicable. Comparing the results of Eqs. (4.106) and (4.107) at the break point of  $Re_s = 100$ , it is found

that the values are not equal, because they are based on different principles. In such cases, the larger value should be taken as a safety factor. [2, 3]

3. The pressure drop in the entrance and exit sections which is shown in Figure 4.14 is affected by bypass but not by leakage. The flow region of the end zones differs from the central cross flow zone in the following respects: (a) the number of tube rows crossed includes the tube rows in the entry or exit window,  $N_{tcw}$ . (b) the leakage streams have not yet developed (entry) or just joined the main stream (outlet) in the end zones, and therefore the leakage correction factor is not applicable. (c) the baffle spacing in the end zones may differ from the central spacing, especially for U-tube bundles. An end zone correction factor  $R_s$  is therefore used. Then the pressure drop in the two end zones  $\Delta p_e$  is [2, 3, 4]

$$\Delta p_e = (\Delta p_{bi}) \left( 1 + \frac{N_{tcw}}{N_{tcc}} \right) R_b R_s \quad (4.108)$$

where  $\Delta p_{bi}$  is calculated in Eq. (4.104),  $R_b$  is the bypass correction factor from Eq. (4.85), and  $R_s$  is the end zone correction factor as defined in Eq. (4.98). For all baffle spacings equal,  $R_s = 2$ .

Finally, the total shell-side pressure drop  $\Delta p_s$ , excluding nozzles, is [2, 3, 4]

$$\Delta p_s = \Delta p_c + \Delta p_w + \Delta p_e \quad (4.109)$$

The pressure drop in the nozzles must be calculated separately and added to the total pressure drop.